The University of Tehran Press

Pollution

Print ISSN: 2383-451X
Online ISSN: 2383-4501

https://jpoll.ut.ac.ir/

Properties of the Nuisance Dust Particles in Sulaymaniyah City, Northeastern Iraq

Shahen Othman Abdulla | Bubak Souri✉

Department of Environmental Sciences, Faculty of Natural Resources, University of Kurdistan, P.O. Box 416 Sanandaj, Iran

Article Info

Article type:
Research Article

Article history:
Received: 7 September 2023
Revised: 7 November 2023
Accepted: 5 December 2023

Keywords:
Environmental Pollutant
Dust-fall Phenomenon
Alkali and Alkaline Earth Metals
Heavy Metals
Middle East

ABSTRACT

Nuisance dust particles have emerged as a significant environmental concern within the Middle Eastern region. The principal aim of this research was to conduct an extensive investigation into the physical and chemical attributes of dust-fall particles located within the city of Sulaymaniyah, northeastern Iraq. Over a period of six months, a total of 72 dust-fall particle samples were systematically gathered from three distinct stations, with intervals of seven days. In addition to quantitative analysis, this study included detailed morphological examinations and mineralogical composition assessments, facilitated through the application of analytical methodologies, including Scanning Electron Microscopy (SEM) and X-Ray Diffraction (XRD). The outcomes of these analytical procedures revealed predominantly irregular shapes of the dust particles, characterized by the presence of quartz and calcite minerals, confirming their natural origin due to wind-driven erosion originating from the arid desert landscapes of Iraq and its neighboring southern and western countries. Moreover, this investigation extended to encompass a comprehensive evaluation of both water-soluble and insoluble fractions, in addition to the overall concentration levels of alkali and alkaline earth metals including sodium (Na), potassium (K), calcium (Ca), and magnesium (Mg). Furthermore, the levels of heavy metals of manganese (Mn), iron (Fe), copper (Cu), and arsenic (As) were investigated. The extent of pollution associated with these elements was assessed through the application of the Geo-accumulation index (Igeo) which revealed that, during the study, calcium, magnesium, and copper demonstrated noticeable levels of contamination within the dust-fall particles of Sulaymaniyah city.

Cite this article: Abdulla, Sh. O., & Souri, B. (2024). Properties of the Nuisance Dust Particles in Sulaymaniyah City, Northeastern Iraq. *Pollution*, 10 (1), 448-465.
https://doi.org/10.22059/POLL.2023.364992.2059

DOI: https://doi.org/10.22059/POLL.2023.364992.2059

INTRODUCTION

Human is constantly exposed to a wide range of environmental pollutants. Pollutions can have long- and short-term harmful effects on human health in various ways (Hampel et al., 2011). One of the problems related to air pollution is the dust-fall phenomenon (Xia et al., 2020; Tong et al., 2023) which currently is occurring intensively in the Middle-East during recent years. Airborne particles originated of natural and human sources have significant effects on climate, environment, human migration and community health (Oudin et al., 2016).

Additionally, dust-fall phenomenon depends on local climatic conditions such as rainfall, temperature, as well as land surface characteristics including vegetation and soil texture (Sun et al., 2003). Wind speed is another important component for dust generation and transportation (Kurosaki and Mikami, 2003). When the wind speed reaches the threshold, dust-fall particles may travel long distances through three processes of creep, jump, and suspension (Jarrah et al., 2020).

*Corresponding Author Email: *bsouri@uok.ac.ir*

Moreover, airborne particles in industrial and densely populated areas may contain particles resulting from consumption of the fossil fuels (Perera, 2018). Dust-fall particles vary in size and are composed of a set of elements with various contents. They are also important because of greater ability to penetrate deep into the human respiratory system (Goudie and Middleton, 2006). Among airborne particles, those larger than 10 micrometers are receiving special attention due to their deposition and durability in man's living places and also adverse effects of them on human health condition (Ghorani-Azam et al., 2016). These particles, if originated from natural sources, mainly contain clay and silt fractions able to absorb various metal compounds (Escudero et al., 2007). They also can be toxic due to potential existence of high concentration of heavy metals (Fang et al., 2007).

Several statistical indices are suggested to evaluate level of elemental pollution in dust particles, including the geo-accumulation index (I_{geo}), the enrichment factor (EF), and the integrated pollution index (IPI) indices (Wei and Yang, 2009; Ghrefat et al., 2010). Furthermore, dust particles may have direct and/or indirect adverse effects on plants, animals and human health such as respiratory problems and cardiovascular diseases (Al-Awadhi and Al-Dousari, 2013; Attiya and Jones, 2020). Therefore, assess of physical and chemical properties of suspended particles is vital to determine the potential impact of these particles on the environment as well as the health of human (Zarasvandi, 2009).

The phenomenon of dust-fall is an important environmental problem that has occurred across Iraqi territories during recent years more frequently. Dust-fall originated of natural resources, especially soil erosion mainly composed of particles from geological deposits, has a significant impact on the physical and chemical composition of air (Xi and Sokolik, 2012), and has become an important environmental concern for Iraqi people in recent years (Attiya et al., 2019) as well as neighboring countries, especially Iran (Tabatabaei et al., 2015; Mihankhah et al., 2020a,b). Iraqi dust-fall phenomenon mainly occurs during summer while the north winds are the most important factors influencing its occurrence (Attiya and Jones, 2020). Varoujan et al. (2013) expressed that the dust-fall phenomenon in the northern half of Iraq apparently originates from the dried lakes, deserts and semi-desert areas in central and southern Iraq, as well as neighboring countries in the west, south and southwest. Awadh (2012) also cited that the deserts of Syria, Jordan, Saudi Arabia and the Sahara in North Africa are the main sources of dust storms that affect different parts of Iraq.

About 40% of Iraqi territories are covered with desert deposits which are considered as the significant sources of dust-fall across the Middle East (Prospero et al., 2002). Since 1990 especially during the last decade desertification in Iraq has increased mainly due to severe drought, construction of dams upstream of the rivers supplying Iraqi plain, political instability and weakness of the central government, military operations and the occurrence of frequent and protracted wars, inadequate afforestation, as well as cessation of water and soil resource conservation measures (Awad, 2003; Ginoux et al., 2012). The aim of this study was to evaluate the quantity and the physicochemical properties of dust-fall particles with a size of larger than 10μm in Sulaymaniyah city in northeastern Iraq.

MATERIAL AND METHODS

Study area and sampling procedure

The study area was Sulaymaniyah city the capital of a prefecture with the very same name in northeastern Iraq having a moderate climate with hot and dry summers and cold winters where rainfall is limited to winters located at N35°34' latitude and E45°24' longitude within an altitude of 882m. Three stations inside Sulaymaniyah city as illustrated in Fig. 1 were decided for sampling of dust-fall particles with a size of 10μm< (PM_{10}) using dust-fall jar method (ASTM, 1982) optimized to follow the strict standards introduced by dust scan (BSI, 1972; DUSTSCAN,

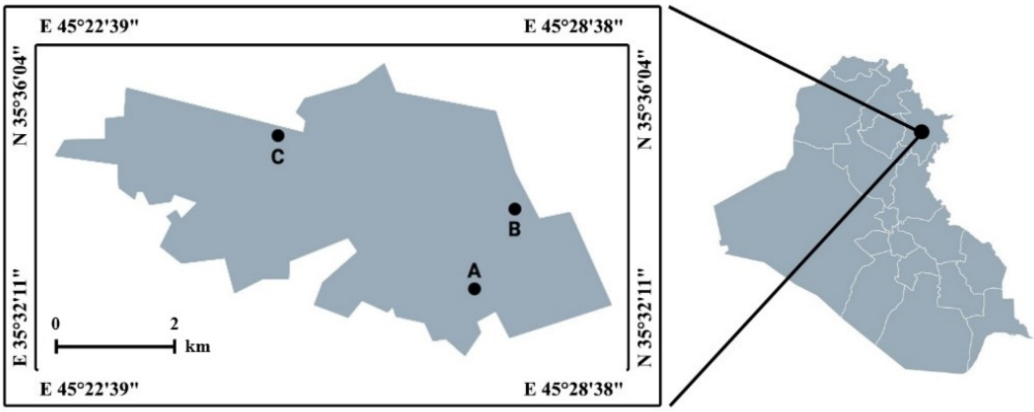

Fig. 1. Iraq map presenting its prefectures and location of Sulaymaniyah city (right) accompanied with the sampling stations of A, B and C inside the city (left)

2011). These three sampling stations chose to obtain an accurate representation of dust-fall situation across the entire city (Naddafi et al., 2006). Dust particles larger than 10 microns (PM_{10}) were systematically sampled over a six-month period, spanning from July 2021 to January 2022, with seven-day intervals between each collection. The method employed for this purpose was the particle accumulation measurement technique, utilizing a specialized accumulation measuring device. Subsequent to each seven-day sampling cycle, the accumulated dust within the glass funnel of the device underwent a dual washing procedure using double-distilled water. This resulting suspension was then carefully transferred into bottles and subsequently conveyed to the laboratory for further analysis. In total, 72 samples were collected during the experiment period.

Physicochemical analyses

Quantity of the dust-fall deposited over the glass funnel of the each device was measured throughout weight difference of the glass funnel before and after of the each seven-day of the sampling period. Then, the dust-fall content deposited over the glass funnel was washed out with double-distilled water into a collector bottle and the suspension obtained for each sample was heated for 2hrs at 95°C to accelerate solving water soluble part of the dust-fall particles (Rajabi and Souri, 2014). Water soluble concentration fractions of alkali metals of Na and K; alkaline earth metals of Ca and Mg; heavy metals of Fe, Mn, Cu and As were measures in the filtered (Whatmann filter paper No.41) liquid obtained (Momani et al., 2000). The water insoluble remains over the filter paper were dissolved by adding 15ml concentrated nitric acid and heating on a Block Digest for 2hrs at 95°C. Following ultrasonic bath for 30min at 50°C the acid digested liquid was passed throughout a filter paper and concentration of water insoluble fractions of Na, K, Ca, Mg, Fe, Mn, Cu and As were measured in the acid digested filtered liquid (Khuzestani and Souri, 2013). Atomic absorption spectroscopy (Phoenix-986) was applied to measure Na, K, Ca, Mg, Fe, Mn by flame and Cu, As by furnace supplement in the above mentioned liquids. Sum of the soluble and insoluble values of the each studied element was considered as the total value of the very same element in the dust-fall samples.

Geo-accumulation index

Geo-accumulation index allows elemental contamination evaluation by comparing present and pre-industrial concentrations of those elements in bottom sediments (Muller, 1969). It might also be used to assess the contamination of diverse environments (Xuan et al., 2004). The following equation represents the index calculation:

Table 1. Pollution levels of the nuisence air particulate materials based on the I_{geo} index

I_{geo}	Contamination level
$I \leq 0$	Uncontaminated
$0 < I < 1$	Uncontaminated to moderately contaminated
$1 < I < 2$	Moderately contaminated
$2 < I < 3$	Moderately/Strongly contaminated
$3 < I < 4$	Strongly contaminated
$4 < I < 5$	Strongly/extremely contaminated
$5 < I$	Extremely contaminated

$$I_{geo} = Log_2\left(\frac{C_n}{1.5B_n}\right)$$

where I_{geo} is the geo-accumulation index, C_n is the measured concentration of the desired element in the collected sample, and B_n is the background concentration of the same element in the earth crust (Turekian and Wedepohl, 1961). The coefficient of 1.5 was used to minimize possible changes in background concentrations caused by geological activities. Table 1 shows the pollution levels of the nuisence air particulate materials based on the I_{geo} index (González-Macías et al., 2006). Among the resources frequently utilized to supply background concentration of the element are the world average shale and soil (Turekian and Wedepohl, 1961).

Meteorological indicators and statistical analyses

The correlation of the studied elements concentration amongst dust-fall samples to the daily average of meteorological parameters, including temperature, relative humidity, wind speed and air pressure (IMO, 2022) was determined using Corr procedure of SAS v.8.2 statistical software, while Microsoft Excel 2021 was used to generate the graphs. The collected data were first examined for normal distribution using the Kolmogorov-Smirnov test, and if required, the data were transformed for normal distribution before analysis. The Crystal Impact Match v1.11 was used to evaluate the X-Ray Diffraction (XRD) spectrum for the samples and the ImageJ software was also used to process the Scanning Electron Microscope (SEM) photographs.

Statistical analyses

The correlation of the studied elements concentration amongst dust-fall samples to the daily average of meteorological parameters, including temperature, relative humidity, wind speed and air pressure (IMO, 2022) was determined using Corr procedure of SAS v.8.2 statistical software, while Microsoft Excel 2021 was used to generate the graphs. The collected data were first examined for normal distribution using the Kolmogorov-Smirnov test, and if required, the data were transformed for normal distribution before analysis.

RESULTS AND DISCUSSION

Quantity of dust-fall

Figure 2 shows the amount of the dust-fall particles of in unit area per week. The average amount of dust-fall collected weekly fluctuates between 0.4 and 6.6 g/m^2. The change in trend of the dust-fall sedimentation was initially upward, then downward, and followed almost a constant trend until the middle of the sampling period. Then, a short-term increase and a sharp decrease were observed, and finally, at the end of the sampling period, there was a sharp

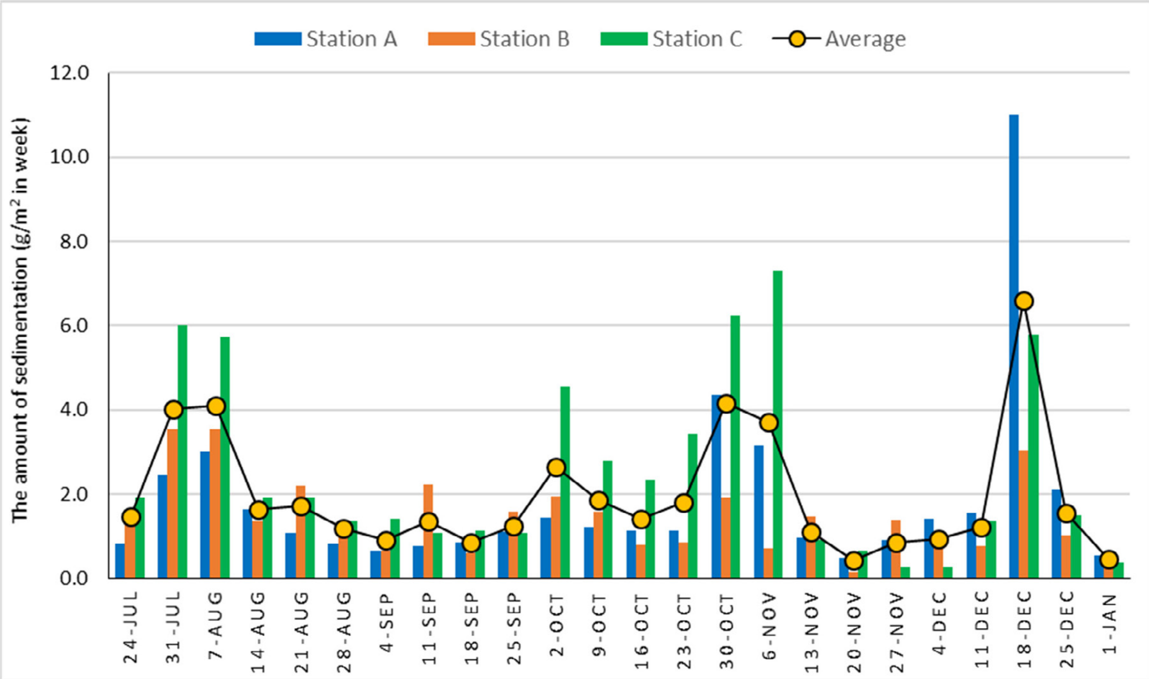

Fig. 2. The amount of dust-fall particles collected at the three sampling stations in Sulaymaniyah city for a weekly six months sampling period during 2021-2022.

increase and decrease. The lowest amount of weekly dust-fall with 0.156 g/m^2 was recorded on November 20 at the B station while the highest amount was recorded on December 18 with 11.01 g/m^2 at the A station. For the first half of the studied period; the highest amount of dust-fall was recorded in the station C but for the second half of the studied period, the amount of dust-fall was the highest in the station A.

Morphology of the dust-fall particles

SEM images of the samples at a scale of 500 nm are shown in Fig. 3. The structure of the particles is angular to spherical state, indicating the effects of natural factors such as wind erosion on formation of these particles (Liu et al., 2005; Wang et al., 2010).

Mineralogical composition

Fig. 4 shows the results of X-ray diffraction (XRD) spectrum analysis for the two samples of dust-fall particles collected at the station B for the weeks 1 (B1) and 21 (B21). As illustrated in the Fig. 4; calcite and quartz were the most abundant among the interpreted minerals.

Levels of alkaline and alkaline-earth metal elements

The summary statistics of the amount of soluble, insoluble and total concentrations for the alkaline metals of Na and K and also alkaline-earth metals of Ca and Mg amongst the dust-fall particles (10µm<) on a weekly basis are presented in Table 2 to 5.

The lowest and highest concentration of soluble sodium with 3.14 mg/g and 30.83 mg/g were observed in the station B, respectively. Also, the lowest and highest concentration of insoluble sodium was found for stations A (0.06 mg/g) and C (7.42 mg/g) while the lowest and highest total concentration of sodium were 3.54 and 37.99 mg/g, respectively, both in B station (Table 2).

The lowest and the highest contents of the soluble potassium fraction was seen in stations C (1.00 mg/g) and A (19.86 mg/g) but for the insoluble fraction in stations B (0.40 mg/g) and C

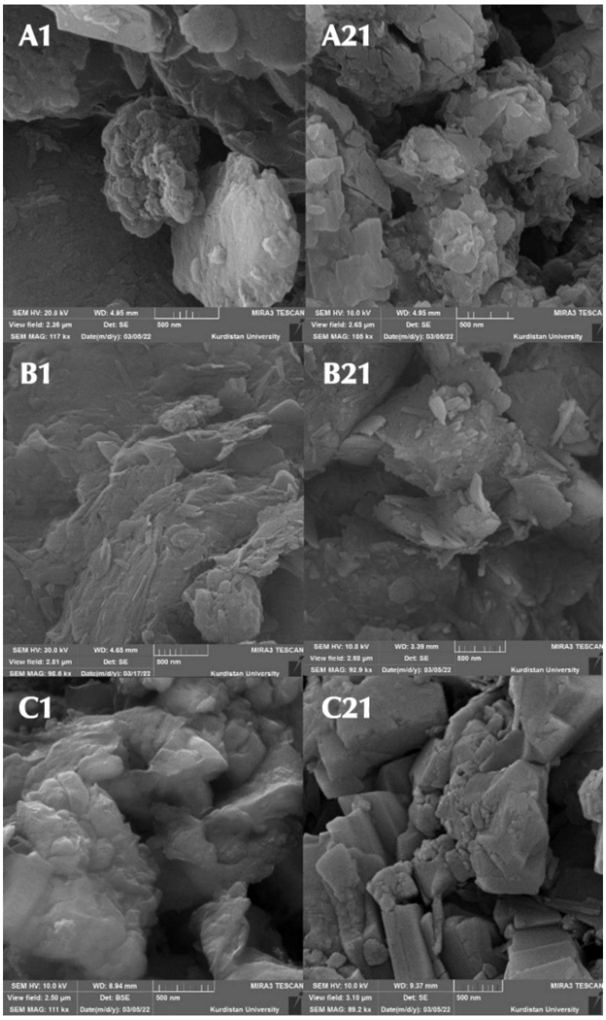

Fig. 3. The SEM images for the collected dust-fall particles sampled at the first and the last weeks of sampling period for the three sampling stations of A, B and C

(3.87 mg/), respectively. For the total potassium; the lowest concentration was recorded with 1.39 mg/g in station B and the highest content with 23.59 mg/g in the station A (Table 3).

The lowest soluble and insoluble concentrations of calcium with 13.48 and 13.38 mg/g were belong to stations A and B but the highest soluble and insoluble concentrations were 273.30 and 267.98 mg/g observed in stations B and C, respectively. The lowest and highest total concentration of calcium were 28.49 and 438.50 mg/g happened in the stations A and B, respectively.

The lowest and the highest contents of soluble fraction of magnesium amongst dust-fall particles measured were 6.52 (station B) and 99.28 mg/g (station A) but for the insoluble fraction were 4.58 (station C) and 140.83 mg/g (station B). The lowest and the highest total concentration of magnesium amongst the dust-fall particles collected were 11.91 mg/g at station C and 243.26 mg/g at station B (Table 5).

Levels of heavy metals

Tables 6 to 9 show the summary statistics of the amount of soluble, insoluble and total concentration of the heavy metals of Mn, Fe, Cu and As amongst the dust-fall particles (<10μm) on a weekly basis.

The lowest and the highest soluble fraction concentrations of manganese amongst the dust-

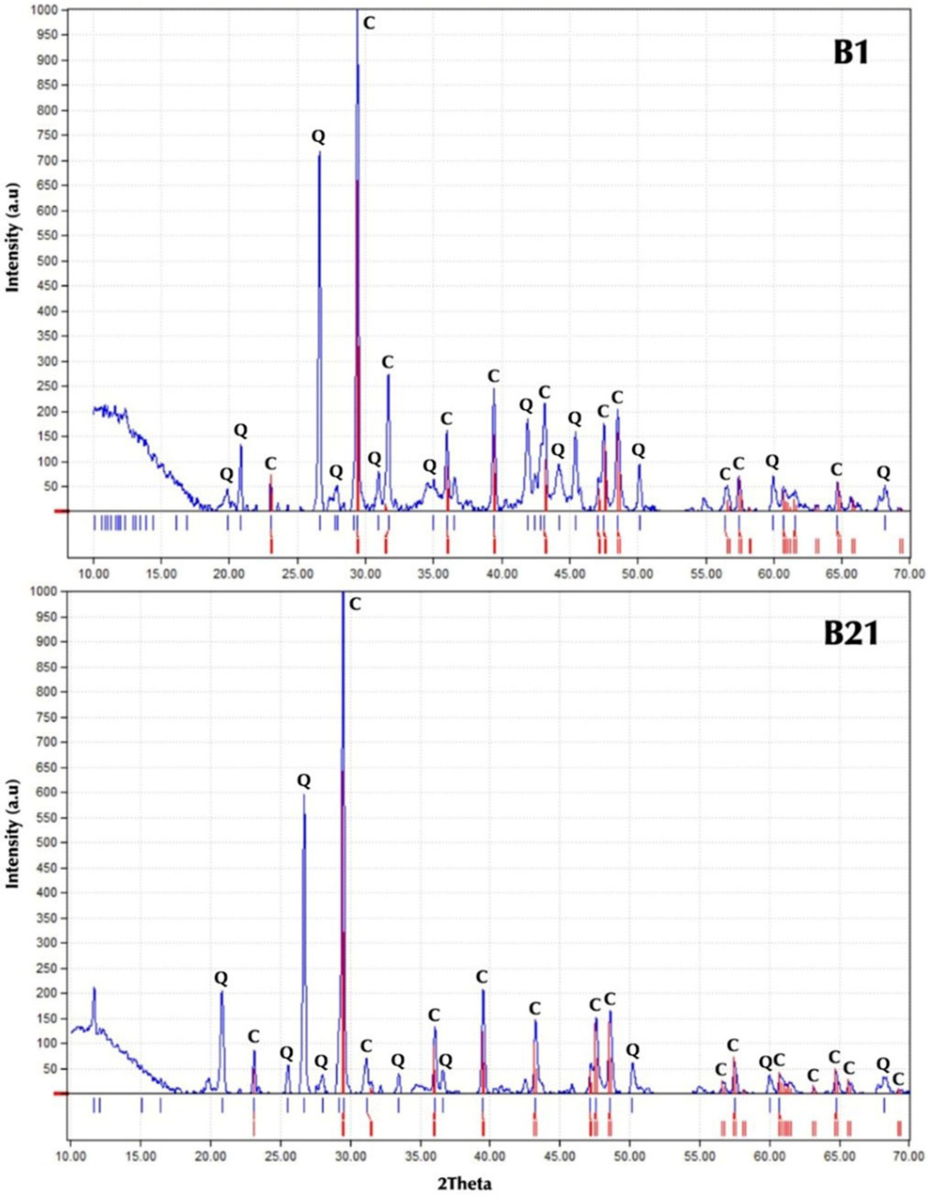

Fig. 4. X-ray diffraction spectrum analysis for the collected dust-fall particles sampled in the sampling station of B at the first (B1) and the last weeks (B21) of sampling period showing Calcite (C) and Quartz (Q) as the most abundant minerals interpreted

Table 2. Summary statistics of the soluble, insoluble and total concentration of Na amongst the dust-fall particles of the three sampling stations (mg/g)

Statistics	Soluble Concentration			Insoluble Concentration			Total Concentration		
	Station			Station			Station		
	A	B	C	A	B	C	A	B	C
Minimum	3.93	3.14	3.85	0.06	0.40	0.51	3.99	3.54	4.36
Maximum	23.16	30.83	12.36	3.64	7.16	7.42	26.80	37.99	19.78
Average	11.31	7.27	7.90	1.95	3.07	3.31	13.26	10.34	11.21
SD	4.97	6.04	2.53	0.98	2.24	1.92	5.95	8.28	4.45

Note: The lowest and the highest values for soluble, insoluble and total concentrations are underlined.

Table 3. Summary statistics of the soluble, insoluble and total concentration of K amongst the dust-fall particles of the three sampling stations (mg/g)

Statistics	Soluble Concentration			Insoluble Concentration			Total Concentration		
	Station			Station			Station		
	A	B	C	A	B	C	A	B	C
Minimum	1.09	0.99	1.00	0.74	0.40	0.69	1.83	1.39	1.69
Maximum	19.86	9.76	8.11	3.73	3.60	3.87	23.59	13.36	11.98
Average	6.31	2.52	3.34	1.82	1.85	2.20	8.13	4.37	5.54
SD	4.09	2.01	1.56	0.72	1.01	0.89	4.81	3.02	2.45

Note: The lowest and the highest values for soluble, insoluble and total concentrations are underlined.

Table 4. Summary statistics of the soluble, insoluble and total concentration of Ca amongst the dust-fall particles of the three sampling stations (mg/g)

Statistics	Soluble Concentration			Insoluble Concentration			Total Concentration		
	Station			Station			Station		
	A	B	C	A	B	C	A	B	C
Minimum	13.48	20.01	21.08	15.01	13.38	14.46	28.49	33.39	35.54
Maximum	228.28	273.30	163.29	195.81	165.20	267.98	424.09	438.50	431.27
Average	59.06	84.43	77.96	85.98	92.84	98.88	145.04	177.27	176.84
SD	48.19	69.41	36.60	43.92	42.03	55.64	92.11	111.44	92.24

Note: The lowest and the highest values for soluble, insoluble and total concentrations are underlined.

Table 5. Summary statistics of the soluble, insoluble and total concentration of Mg amongst the dust-fall particles of the three sampling stations (mg/g)

Statistics	Soluble Concentration			Insoluble Concentration			Total Concentration		
	Station			Station			Station		
	A	B	C	A	B	C	A	B	C
Minimum	10.83	6.52	7.33	8.31	8.96	4.58	19.14	15.48	11.91
Maximum	99.28	93.43	82.26	107.53	140.83	51.41	206.81	243.26	133.67
Average	36.72	35.93	35.23	58.10	46.33	22.02	94.82	82.26	57.25
SD	21.48	19.80	17.57	27.60	27.41	10.98	49.08	47.21	28.55

Note: The lowest and the highest values for soluble, insoluble and total concentrations are underlined.

Table 6. Summary statistics of the soluble, insoluble and total concentration of Mn amongst the dust-fall particles of the three sampling stations (mg/g)

Statistics	Soluble Concentration			Insoluble Concentration			Total Concentration		
	Station			Station			Station		
	A	B	C	A	B	C	A	B	C
Minimum	0.01	0.01	0.02	0.25	0.15	0.23	0.26	0.16	0.25
Maximum	0.27	0.27	0.35	1.17	1.25	1.28	1.44	1.52	1.63
Average	0.09	0.11	0.16	0.43	0.51	0.70	0.52	0.62	0.86
SD	0.08	0.07	0.10	0.22	0.26	0.28	0.30	0.33	0.38

Note: The lowest and the highest values for soluble, insoluble and total concentrations are underlined.

fall samples were 0.01 mg/g (station A) and 0.35 mg/g (station C) while for insoluble fraction were 0.15 mg/g (station B) and 1.28 mg/g (station C), respectively. The station B had the lowest total concentration of manganese with 0.16 mg/g but station C had the highest concentration

Table 7. Summary statistics of the soluble, insoluble and total concentration of Fe amongst the dust-fall particles of the three sampling stations (mg/g)

Statistics	Soluble Concentration			Insoluble Concentration			Total Concentration		
	Station			Station			Station		
	A	B	C	A	B	C	A	B	C
Minimum	0.08	0.10	0.04	1.10	2.81	2.31	1.18	2.91	2.35
Maximum	1.68	2.66	4.49	14.89	33.87	38.45	16.57	36.53	42.94
Average	0.47	0.80	0.97	11.37	15.25	19.89	11.84	16.05	20.86
SD	0.40	0.68	0.89	3.24	7.86	9.37	3.64	8.54	10.26

Note: The lowest and the highest values for soluble, insoluble and total concentrations are underlined.

Table 8. Summary statistics of the soluble, insoluble and total concentration of Cu amongst the dust-fall particles of the three sampling stations (mg/g)

Statistics	Soluble Concentration			Insoluble Concentration			Total Concentration		
	Station			Station			Station		
	A	B	C	A	B	C	A	B	C
Minimum	0.03	0.01	0.02	0.01	0.01	0.02	0.04	0.02	0.04
Maximum	0.84	0.52	0.48	0.30	0.41	0.25	1.14	0.93	0.73
Average	0.19	0.19	0.20	0.13	0.15	0.13	0.32	0.34	0.33
SD	0.16	0.13	0.13	0.07	0.10	0.07	0.23	0.23	0.20

Note: The lowest and the highest values for soluble, insoluble and total concentrations are underlined.

Table 9. Summary statistics of the soluble, insoluble and total concentration of As amongst the dust-fall particles of the three sampling stations (µg/g)

Statistics	Soluble Concentration			Insoluble Concentration			Total Concentration		
	Station			Station			Station		
	A	B	C	A	B	C	A	B	C
Minimum	0.009	0.004	0.007	0.008	0.000	0.009	0.017	0.004	0.016
Maximum	0.323	0.357	0.274	0.158	0.154	0.236	0.481	0.511	0.510
Average	0.165	0.148	0.135	0.078	0.075	0.082	0.243	0.223	0.217
SD	0.099	0.100	0.077	0.039	0.044	0.058	0.138	0.144	0.135

Note: The lowest and the highest values for soluble, insoluble and total concentrations are underlined.

with 1.63 mg/g (Table 6).

The lowest and highest soluble concentration of iron with 0.04 mg/g and 4.49 mg/g were observed in station C while for insoluble fraction the lowest and the highest contents were 1.10 mg/g (station A) and 38.45 mg/g (station C). The total iron concentrations fluctuated between minimum of 1.18 mg/g for station A and maximum of 42.94 mg/g for station C (Table 7).

When copper concentration considered the lowest and highest soluble concentration of copper with 0.01 mg/g and 0.84 mg/g were belonged to station B and A, respectively. The lowest and highest insoluble concentration of copper with 0.01 mg/g and 0.41 mg/g belong to station B both. Moreover, stations B and A with 0.02 mg/g and 1.14 mg/g had the lowest and the highest total concentration of copper, respectively (Table 8).

The amount of soluble arsenic was lowest (0.004 µg/g) and highest (0.357 µg/g) both for station B while the lowest and the highest values for insoluble fraction of arsenic were 0.000

µg/g and 0.236 µg/g for station B and A, respectively. The lowest and highest total concentration of arsenic were 0.004 µg/g and 0.511 µg/g recorded in station B (Table 9).

Contamination levels of alkaline and alkaline-earth metals

Geo-accumulation index (I_{geo}) average values for alkaline and alkaline-earth metals of Na, K, Ca and Mg amongst dust-fall particles sampled from the three sampling stations of the study area during the six months of sampling period are shown in Fig. 5. The results showed that the concentration of potassium in the air of Sulaymaniyah city was not at the contaminating level (-4.59 to -1.82) while sodium concentration was in the level of uncontaminated to moderately contaminated (-1.59 to 0.62). Instead, the most contaminating amounts of alkaline and alkaline-earth metals were belonged to calcium and magnesium resulting in I_{geo} index to fluctuate between uncontaminated and strongly contaminated contamination level (-0.03 to 3.50 for calcium and -0.50 to 2.59 for magnesium). However, the contamination levels of these two alkaline-earth metals were assessed as uncontaminated on December 18 sampling.

Contamination levels of heavy metals

Fig. 6 illustrates geo-accumulation index (I_{geo}) average values for heavy metals of Mn, Fe, Cu and As amongst dust-fall particles sampled from the three sampling stations of the study area during the six months of sampling period. The index values for manganese, iron and arsenic amongst the dust-fall particles of study area was at the uncontaminated level. Nevertheless, the geo-accumulation index values for copper amongst the dust-fall particles of the study area fluctuated between moderately contaminated to strongly contaminated levels except for one sampling at 18th December 2022 with the uncontaminated level.

Gherboudj et al. (2017) characterized the spatial and temporal variability of the dust emission potential of the Middle East and North Africa according to three scales: low, medium and high dust emission zones. Areas of high and medium dust emission in North Africa include the

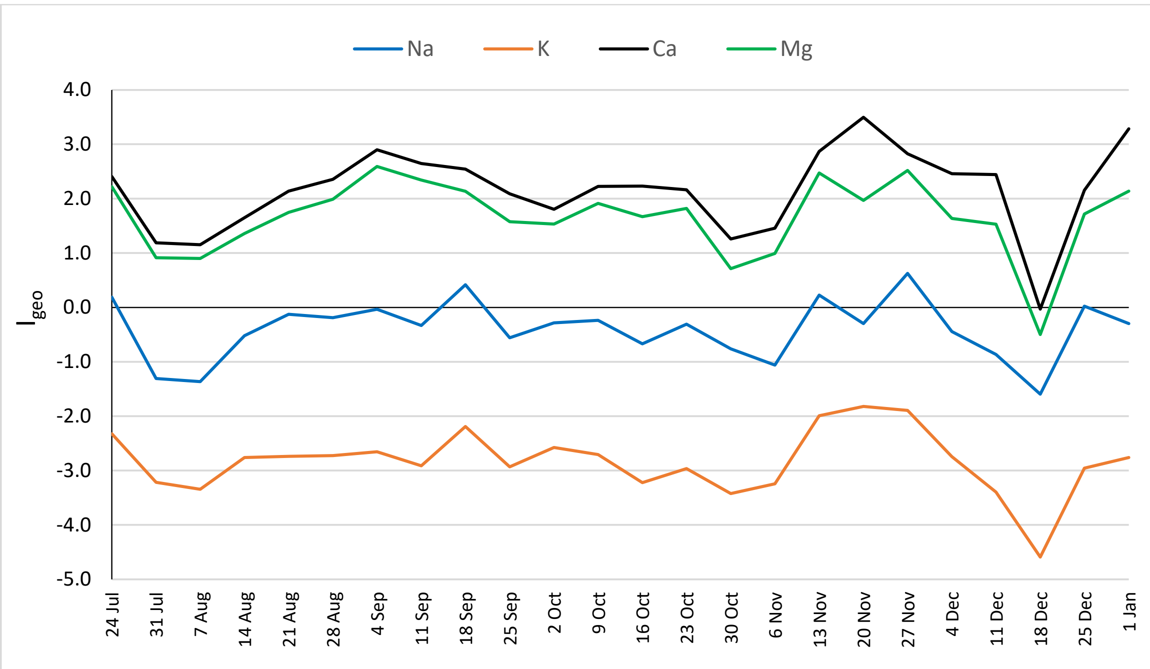

Fig. 5. Geo-accumulation index (I_{geo}) average values for alkaline and alkaline-earth metals of Na, K, Ca and Mg amongst dust-fall particles sampled from the three sampling stations of the study area for a weekly six months sampling period during 2021-2022..

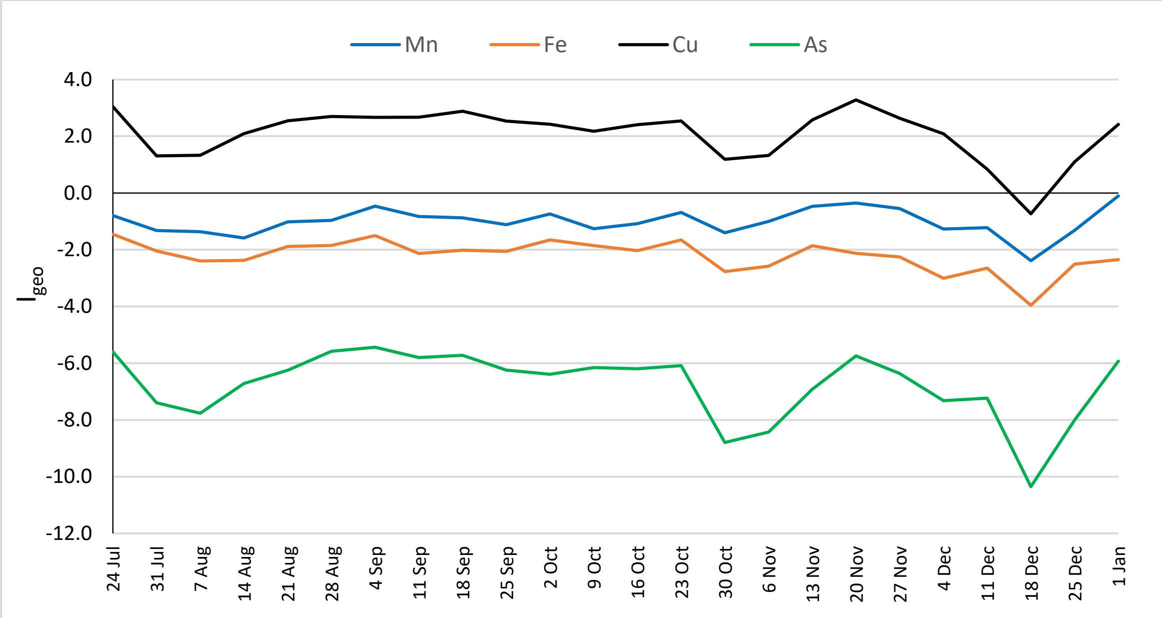

Fig. 6. Geo-accumulation index (I_{geo}) average values for heavy metals of Mn, Fe, Cu and As amongst dust-fall particles sampled from the three sampling stations of the study area for a weekly six months sampling period during 2021-2022.

countries of Chad, Niger, Mauritania, western Sahara, western and northern Algeria, southern Tunisia, northwestern and central Libya, central Egypt, Sudan, and the Horn of Africa. In the Middle East, the countries of Jordan, Syria, eastern Iraq and the Arabian Peninsula were among the areas with high and medium dust emissions. In addition, the central regions of Iran, western Afghanistan, southwestern Pakistan, and western India are sources of dust production (Querol et al., 2019). The Eastern Mediterranean region, especially the country of Iraq, suffers from periods of sand and dust storms that have been reported more frequently in the past decades (Amarloei et al., 2020; Fountoukis et al., 2020; Saeifar and Alijani, 2019). Climate change and its consequences through desertification, deforestation, destruction of wetlands, population growth and human emissions, food insecurity and water shortage have been mentioned among the factors affecting the increase in the frequency of sand and dust storms in the Eastern Mediterranean region (Amiraslani and Dragovich, 2011; Notaro et al., 2015; Rezazadeh et al., 2013). Notaro et al. (2015) showed that the eastern Mediterranean region has experienced warming and drying since the beginning of the century, leading to an increase in the potential of damage to the environment of Iraq and Syria. In the Middle East, especially in the Arabian Peninsula, a significant change in the activities of fine dust has been reported with a sudden change from the inactive dust period (1998-2005) to the active dust period (2007-2013) (Aba et al., 2018), which was associated with climate change and global warming effects in the 2000s (Doronzo et al., 2016; Notaro et al., 2015). The increase in dust period and dust concentration in the upper atmosphere has a significant effect on albedo and shortwave radiation in Arab regions, leading to higher surface reflectance (Satheesh et al., 2006), especially in Iraq (Al-Hemoud et al., 2020) and Kuwait (Al-Dousari et al., 2019). The fine dust resulting from this event causes direct and indirect adverse effects for animals, plants and human health on a regional scale and the areas around the sampling sites will not be an exception to this rule.

Analysis of SEM images for the samples collected from all three stations in the first and last week of the study period showed that most of the dust-fall particles are formed from the adhesion of smaller particles. This characteristic of the particles can indicate the accumulation of calcite and quartz minerals, which was also confirmed by X-ray diffraction analysis. The samples collected in the 1st and the 21st week for stations A and B show slight differences. The 21st week samples of the three stations were collected in winter while the 1st week samples belonged to summer. The dust particles in the samples collected during summer were larger in size, which may indicate that the particles in the summer were having much natural behavior compared to the winter and may have a desert origin (Furman, 2003). Also, the samples collected in the winter, especially for the station C have elongated sharp edges implying that these particles originated from closer sources and probably entered the air more probably due to human activities (Kuo and Shen, 2010). Diameter of the particles marked in the images were very helpful in determining the type of mineral as particles with almost spherical or irregular shapes were mostly suspicious to be quartz whereas larger crystals were considered as albite mineral (Zarasvandi et al., 2019). According to the abovementioned facts and considering the SEM images, it can be concluded that the particles in the air of the study area were of calcite and quartz type, and these results were also confirmed by X-ray diffraction analysis. In a study conducted by Bashiri Khuzestani and Souri (2013), the results showed that the particles in the dust-fall in Sanandaj city, western Iran, are often angular non-spherical and accordingly wind erosion was recognized as the reason for changing the shape of dust particles. In another study related to the shape of dust particles in the air of same city; Rajabi and Souri (2014) reported that these particles had irregular shapes that could be caused through transportation by wind. Mosavi and Pourkhabaz (2017) reported that the particles in the air of Birjand city, northeastern Iran, were spherical, irregular, elongated, crystalline, or rhombic mainly consisted with aluminosilicate clay and quartz. In the study conducted by Zarasvandi et al. (2013), the observation of spherical, irregular, stretched and prismatic shapes, crystal macule or rhombus in the air of Khuzestan province, southwestern Iran, was reported, which respectively represented aluminosilicate clay particles, quartz, gypsum and calcite in round particles. The results of X-ray diffraction analysis showed that the particles of dust-fall in Sulaymaniyah are mostly composed of calcite and quartz. Wagner (2009) suggested that if the accumulated dust is calcareous and provides sufficient calcium carbonate ($CaCO_3$), calcic horizons will form over time. Furthermore, Dimmitt et al. (2015) suggested that presence of calcium in dust and rain are the main sources of calcic horizons that are mostly observed in desert soils. On the other hand, Kraimer and Monger (2009) and also Zamanian et al. (2016) pointed out that although soils are the third largest source of carbon (organic and inorganic form) on earth while they probably also absorb atmospheric carbon. Previous studies have emphasized that quartz has toxic properties, which can vary significantly depending on the surface characteristics of the quartz mineral (blocked fractured surface quartz) (Creutzenberg et al., 2008). Donaldson and Borm (1998) mentioned that the toxic effect of quartz is connected to surface reactivity and may vary significantly depending on the origin of the quartz sample. These researchers also showed that the mechanism of quartz toxicity involves the production of free radicals and reactive oxygen species. Considering that the sampling stations in the present study are close to the cement factories; the relatively high percentage of quartz can be attributed to the activity of these factories. Al-dabbas et al. (2011) observed similar compounds in samples collected from the central and southern regions of Iraq, although the amounts of those compounds were different comparing to the current study. In a similar study on the mineralogical classification of dust particles in Asia, Jeong (2008) found minerals including clay aggregates often mixed with nano-sized calcite, quartz, plagioclase, coarse calcite, potassium feldspar, muscovite, chlorite, kaolinite, amphibole, gypsum, iron and titanium oxides partially or completely bound to clay-sized mineral grains. In another study, Bashiri Khuzestani and Souri (2013) reported that the main minerals that make up the dust-fall particles in the air of Sanandaj city are quartz and calcite, which was in agreement with the results of the current study. These results were also reported by Rajabi and Souri (2014) on dust-fall particles in the air of Sanandaj city, which can be a confirmation of the same origin of nuisance air particulate materials for the two cities of Sanandaj (western Iran) and Sulaymaniyah (northeastern Iraq).

Among the alkaline and alkaline-earth metals studied calcium was the most abundant compared to sodium, potassium and magnesium. After calcium, magnesium, potassium and sodium were the most abundant, respectively. Among the elements that make up the earth's crust, calcium and magnesium are ranked fifth and eighth, respectively. Airborne particles have different chemical compositions and the range of these compounds can be very wide. The presence of these elements in dust-fall particles is a proof of their desert origin (Wang et al., 2010). It should be noted that the type of soil in the studied area and neighboring regions contain large amounts of lime, which explains the presence of large amounts of calcium in the air of Sulaymaniyah city. In addition, many cement factories have been built around Sulaymaniyah city in recent years and the activity of these factories plays an important role in spreading particles of calcium and magnesium carbonate minerals which are common among the soils of the region (Dabiri, 2015). It has been documented that suspended particles in the air are divided into two categories: desert and industrial. Industrial particles are smaller than desert particles and heavy metals form a large part of them. But desert particles are originated from soil erosion which is the main factor of their diffusion in the atmosphere and mostly are circular due to erosion in their transportation path. Calcium, magnesium and other calcareous compounds are among the main components of desert particles, and according to this fact, the effects of desert particles on health are much less than industrial particles (Esmaeili Sari, 2003). Thus, the study of elemental composition of dust-fall particles including soluble and insoluble fractions of them can be very vital for the societies affected. The Sulaymaniyah city is located in the direction of the north winds, and these strong winds, which are the result of the instability of the air in the countries of Iraq and Saudi Arabia, are responsible for the transfer of dust from the surrounding deserts, especially the central desert of Iraq and the Rub' al-Khali desert in Saudi Arabia (Majid and Kassim, 2018; Attiya and Jones, 2020).

In the present study, iron had the highest concentration among the studied heavy metals, followed by manganese, copper and arsenic with potentially adverse effects on the environment (Omar, 2005). Among the factors affecting the release of these metals in the atmosphere are soil erosion, volcanic activities, climatic factors and human activities (Thakur et al., 2004). Furthermore, the deserts of the Middle East are known as one of the important sources of iron emission in the atmosphere (Wang et al., 2010), which explains the presence of a significant amount of iron due to the location of the Sulaymaniyah city.

Clay minerals are one of the most effective fractions of dust-fall particles in the transfer, absorption and diffusion of compounds throughout the natural environments. Weak van der Waals bonds are responsible for the formation of the chemical structure of these minerals, which are broken by various meteorological factors such as wind speed and temperature, and as a result, the production and transportation of dust increases (Dube et al., 2001). These particles are also composed of water-soluble compounds which can remain in the atmosphere in solid form or in the form of very fine droplets, and with the increase in air humidity, their amounts per unit area also increase (Barkan and Alpert, 2008).

In a similar study conducted by Bashiri Khuzestani and Souri (2013), the average total concentration of alkaline and alkaline-earth metals in Sanandaj air dust-fall particles, including calcium, sodium, potassium, and magnesium was 68.84, 12.45, 5.74 and 2.13 mg/m^2 per month, respectively. Furthermore, these researchers reported total concentration of 11.11, 0.42, 0.045, and 0.014 mg/m^2 for iron, manganese, copper and arsenic, respectively, which were in consistent with the results of present study in terms of the order of abundance. In addition, Rajabi and Souri (2014) reported that the average total concentration of calcium, sodium and potassium in the air of Sanandaj city was 272.92, 138.47 and 85.08 μg/g, respectively. Moreover, these researchers reported the average total concentration of iron, manganese, copper and arsenic as

274.64, 22.44, 13.66 and 5.53 μg/g, respectively. The similarity of the concentration of these elements in the air of Sanandaj and Sulaymaniyah indicates the same origin of these elements in the dust-fall particles of these two cities, which can be explained by the relatively close distance between these two cities. Majid and Kassim (2018) also studied iron concentration values in the dust-fall particles of Sulaymaniyah city and reported that the average iron concentration of samples collected from 16 different stations was 2.24 g/kg.

The results of I_{geo} index revealed that among the eight studied elements, only copper, calcium and magnesium were classified as contaminant, and other elements were either not contaminant or showed a negligible level of contamination. The highest level of air pollution in Sulaymaniyah city occurred in November, especially in the last week, but it seems that the level of air contamination has decreased with the decrease in temperature and increase in humidity. The presence of large amounts of copper in the air can irritate the nose, mouth, and eyes and cause headaches, stomachaches, dizziness, vomiting, and diarrhea. Absorption of excessive amounts of copper may cause liver and kidney damage and even death (Zhang et al., 2021). Inhaling calcium can irritate the lungs and cause coughing and shortness of breath. Exposure to large amounts of calcium may cause fluid to accumulate in the lungs (pulmonary edema) or severe shortness of breath, which is considered an emergency. Furthermore, inhalation of magnesium oxide can irritate the eyes and nose and exposure to large amounts of magnesium can cause metal fume fever (Greenberg and Vearrier, 2015). In the study of the levels of heavy metals in the air of Sanandaj city, Bashiri Khuzestani and Souri (2013) reported that iron and manganese were uncontaminated, but copper and arsenic were contaminated at some times of the experiment and showed moderately uncontaminated at some times. Rajabi and Souri (2014) reported that the copper and silver had the highest contamination in the three studied stations, and after these two elements, the average level of nickel and arsenic contamination was observed. Nevertheless, these researchers considered the amounts of other studied metals as uncontaminated. MalAmiri et al., (2022) reported that calcite was the dominant mineral in dust-fall samples collected from air of Khuzestan province, southwestern Iran, with a high quartz and dolomite fraction. They also reported that the most abundant major compounds were SiO_2 and CaO, while Cl, Ba, Sr, Pb, Ni, Zn, Cr, V were the main trace elements. Furthermore, these researchers suggested that all samples were found to be contaminated by heavy metals due to prior war-related materials, oil and gas extraction, and emissions from polluting industries.

CONCLUSION

Origin of nuisance dust particles in this study was mostly natural caused by wind erosion throughout central and southern deserts of Iraq and also Rub’ al-Khali desert of southern neighboring countries. Amongst the dust particles studied only elements of calcium, magnesium and copper showed some levels of contamination which was a reconfirmation of natural origin of nuisance dust in Sulaymaniyah city mostly resulted from wind erosion of soil and surface geological formations across the region. In order to decrease the chance of the dust particles to reach the city planting trees and making green belt barriers against the dust-fall invasion might be beneficial. Further researches are recommended to acquire a comprehensive overview of green belt barrier behavior and its efficiency to reduce nuisance dust particles entering the city.

GRANT SUPPORT DETAILS

The present research did not receive any financial support.

CONFLICT OF INTEREST

The authors declare that there is not any conflict of interest regarding the publication of this manuscript. In addition, the ethical issues, including plagiarism, informed consent, misconduct, data fabrication and/ or falsification, double publication and/or submission, and redundancy has been completely observed by the authors.

LIFE SCIENCE REPORTING

No life science threat was practiced in this research.

REFERENCES

Aba, A., Al-Dousari, A. M., & Ismaeel, A. (2018). Atmospheric deposition fluxes of 137Cs associated with dust fallout in the northeastern Arabian Gulf. Journal of Environmental Radioactivity, 192, 565–572.

Al-Awadhi, J. M., & Al-Dousari, A. M. (2013). Morphological characteristics and development of coastal nabkhas, north-east Kuwait. International Journal of Earth Sciences, 102(3), 949–958.

Al-dabbas, M., Abbas, M. A., & Khafaji, R. A. (2011). The Mineralogical and Micro-Organisms Effects of Regional Dust Storms over Middle East Region. International Journal of Water Resources and Arid Environments, 1(2).

Al-Dousari, A., Al-Nassar, W., Al-Hemoud, A., Alsaleh, A., Ramadan, A., Al-Dousari, N., & Ahmed, M. (2019). Solar and wind energy: Challenges and solutions in desert regions. Energy, 176, 184–194.

Al-Hemoud, A., Al-Dousari, A., Al-Dashti, H., Petrov, P., Al-Saleh, A., Al-Khafaji, S., Behbehani, W., Li, J., & Koutrakis, P. (2020). Sand and dust storm trajectories from Iraq Mesopotamian flood plain to Kuwait. Science of the Total Environment, 710.

Amarloei, A., Fazlzadeh, M., Jafari, A. J., Zarei, A., & Mazloomi, S. (2020). Particulate matters and bioaerosols during Middle East dust storms events in Ilam, Iran. Microchemical Journal, 152.

Amiraslani, F., & Dragovich, D. (2011). Combating desertification in Iran over the last 50 years: An overview of changing approaches. In Journal of Environmental Management. Vol. 92, Issue 1, 1–13.

ASTM D1739-98 (2010). Standard Test Method for Collection and Measurement of Dustfall (Settleable Particulate Matter). http://www.astm.org/Standards/D1739.htm

Attiya, A. A., & Jones, B. G. (2020). Assessment of mineralogical and chemical properties of airborne dust in Iraq. SN Applied Sciences, 2(9).

Attiya, A. A., Jones, B. G., & Marx, S. (2019). Spatial–temporal analysis of Aerosol Index (AI) distribution and some climatic factors: case study from Iraq, 1980–2015. Modeling Earth Systems and Environment, 5(1), 203–216.

Attiya, A. A., & Jones, B. G. (2020). Climatology of Iraqi dust events during 1980–2015. SN Applied Sciences, 2, 845.

Awadh, S. M. (2012). Geochemistry and mineralogical composition of the airborne particles of sand dunes and dust storms settled in Iraq and their environmental impacts. Environmental Earth Sciences, 66(8), 2247–2256.

Barkan, J., & Alpert, P. (2008). Synoptic patterns associated with dusty and non-dusty seasons in the Sahara. Theoretical and Applied Climatology, 94(3–4), 153–162.

Bashiri Khuzestani, R., & Souri, B. (2013). Evaluation of heavy metal contamination hazards in nuisance dust particles, in Kurdistan Province, western Iran. Journal of Environmental Sciences, 25(7), 1346–1354.

Creutzenberg, O., Hansen, T., Ernst, H., Muhle, H., Oberdorster, G., & Hamilton, R. (2008). Toxicity of a quartz with occluded surfaces in a 90-day intratracheal instillation study in rats. Inhalation Toxicology, 20(11).

Dabiri, M. (2015). Environmental pollution: air - water - soil - sound. Etihad Publications. Tehran, Iran. (in Persian)

Donaldson, K., & Borm, P. J. A. (1998). The quartz hazard: A variable entity. Annals of Occupational Hygiene, 42(5).

Doronzo, D. M., Al-Dousari, A., Folch, A., & Dagsson-Waldhauserova, P. (2016). Preface to the Dust Topical Collection. In Arabian Journal of Geosciences. Vol. 9, Issue 6.
Dube, A., Zbytniewski, R., Kowalkowski, T., Cukrowska, E., & Buszewski, B. (2001). Adsorption and Migration of Heavy Metals in Soil. Polish Journal of Environmental Studies, 10(1), 1–10.
Escudero, M., Querol, X., Pey, J., Alastuey, A., Pérez, N., Ferreira, F., Alonso, S., Rodríguez, S., & Cuevas, E. (2007). A methodology for the quantification of the net African dust load in air quality monitoring networks. Atmospheric Environment, 41(26), 5516–5524.
Esmaeili Sari, A. (2003). Pollutants, health and standards in the environment. Naghshe Mehr Publications. Tehran, Iran. (in Persian)
Fang, G. C., Wu, Y. S., Lee, W. J., Chou, T. Y., & Lin, I. C. (2007). Study of ambient air particulates pollutants near Taichung airport sampling site in central Taiwan. Journal of Hazardous Materials, 144(1–2), 492–498.
Fountoukis, C., Harshvardhan, H., Gladich, I., Ackermann, L., & Ayoub, M. A. (2020). Anatomy of a severe dust storm in the middle east: Impacts on aerosol optical properties and radiation budget. Aerosol and Air Quality Research, 20(1), 155–165.
Furman H. K. H. (2003). Dust storms in the Middle East: Sources of origin and their temporal characteristics. Indoor and Built Environment, 12(6), 419-426.
Gerivani, H., Lashkaripour, G. R., Ghafoori, M., & Jalali, N. (2011). The source of dust storm in Iran: A case study based on geological information and rainfall data. Carpathian Journal of Earth and Environmental Sciences, 6(1), 297–308.
Gherboudj, I., Naseema Beegum, S., & Ghedira, H. (2017). Identifying natural dust source regions over the Middle-East and North-Africa: Estimation of dust emission potential. In Earth-Science Reviews. Vol. 165, 342–355.
Ghorani-Azam, A., Riahi-Zanjani, B., & Balali-Mood, M. (2016). Effects of air pollution on human health and practical measures for prevention in Iran. Journal of Research in Medical Sciences, 21, 65.
Ghrefat, H., Abu-Rukah, Y., & Rosen M.A. (2010). Application of geoaccumulation index and enrichment factor for assessing metal contamination in the sediments of Kafrain Dam, Jordan. Environ Monitoring and Assessment, 178(1-4), 95–109.
Ginoux, P., Prospero, J. M., Gill, T. E., Hsu, N. C., & Zhao, M. (2012). Global-scale attribution of anthropogenic and natural dust sources and their emission rates based on MODIS Deep Blue aerosol products. Reviews of Geophysics, 50(3).
González-Macías, C., Schifter, I., Lluch-Cota, D.B., & Hernández-Vázquez, S. (2006). Distribution, Enrichment and Accumulation of Heavy Metals in Coastal Sediments of Salina Cruz Bay, México. Environmental Monitoring and Assessment, 118, 211–230.
Goudie, A. S., & Middleton, N. J. (2006). Desert dust in the global system. In Desert Dust in the Global System.
Greenberg, M. I., & Vearrier, D. (2015). Metal fume fever and polymer fume fever. In Clinical Toxicology, (53)4.
Hampel, R., Lepeule, J., Schneider, A., Bottagisi, S., Charles, M. A., Ducimetière, P., Peters, A., & Slamab, R. (2011). Short-term impact of ambient air pollution and air temperature on blood pressure among pregnant women. Epidemiology, 22(5), 671–679.
IMO. (2022). Iraqi Meteorological Organization.
Jarraha, M., Mayela, S., Tatarkob, J., Funkc, R., & Kuka, K. (2020). A review of wind erosion models: Data requirements, processes, and validity. CATENA, 187, 104388.
Kraimer, R. A., & Monger, H. C. (2009). Carbon isotopic subsets of soil carbonate-A particle size comparison of limestone and igneous parent materials. Geoderma, 150(1–2).
Kuo, H., & Shen, H. (2010). Indoor and outdoor $PM_{2.5}$ and PM_{10} concentrations in the air during a dust storm. Building and Environment, 45(3), 610-614.
Kurosaki, Y., & Mikami, M. (2003). Recent frequent dust events and their relation to surface wind in East Asia. Geophysical Research Letters, 30(14).
Liu, W. H., Zhao, J. Z., Ouyang, Z. Y., Sorderlund, L., & Liu, G. H. (2005). Impacts of sewage irrigation on heavy metal distribution and contamination in Beijing, China. Environment International, 31(6), 805–812.
Majid, S. N., & Kassim, J. K. (2018). Mineralogical and Chemical Characterization of Settleable Dustfall in Sulaimani City, Kurdistan Region, Iraq. Soil Science, 183(2).

MalAmiri, N., Rashki, A., Hosseinzadeh, S. R., & Kaskaoutis, D. G. (2022). Mineralogical, geochemical, and textural characteristics of soil and airborne samples during dust storms in Khuzestan, southwest Iran. Chemosphere, 286, 131879.
Mihankhah, T., Saeedi, M., Karbassi, A. (2020a). Contamination and cancer risk assessment of polycyclic aromatic hydrocarbons (PAHs) in urban dust from different land uses in the most populated city of Iran. Ecotoxicology and environmental safety, 187, 109838.
Mihankhah, T., Saeedi, M., Karbassi, A. (2020b). comparative study of elemental pollution and health risk assessment in urban dust of different land uses in Tehran's urban area. Chemosphere 241, 124984.
Momani, K.A., Jiries, A.G., & Jaradat, Q.M. (2000). Atmospheric deposition of Pb, Zn, Cu and Cd in Amman, Jordan. TURK Journal of Chemistry, 24, 231–237.
Mosavi, H., & Pourkhabaz, A. R. (2017). Dust source identification using physical-chemical characterization in Birjand. Journal of Environmental Geology, 11(38), 1-9.
Muller, G. (1969). Index of geo-accumulation in sediments of the Rhine River. Geological Journal, 2(3), 108–118.
Naddafi, K., Nabizadeh, R., Soltanianzadeh, Z., & Ehrampoosh, M. H. (2006). Evaluation of dustfall in the air of yazd. Iranian Journal of Environmental Health Science, 3(3), 161–168.
Notaro, M., Yu, Y., & Kalashnikova, O. V. (2015). Regime shift in arabian dust activity, triggered by persistent fertile crescent drought. Journal of Geophysical Research, 120(19), 10229–10249.
Omar, A. H., Won, J. G., Winker, D. M., Yoon, S. C., Dubovik, O., & McCormick, M. P. (2005). Development of global aerosol models using cluster analysis of Aerosol Robotic Network (AERONET) measurements. Journal of Geophysical Research, 110, 1–14.
Oudin, A., Forsberg, B., Adolfsson, A. N., Lind, N., Modig, L., Nordin, M., Nordin, S., Adolfsson, R., & Nilsson, L. G. (2016). Traffic-related air pollution and dementia incidence in Northern Sweden: A longitudinal study. Environmental Health Perspectives, 124(3), 306–312.
Perera, F. (2018). Pollution from Fossil-Fuel Combustion is the Leading Environmental Threat to Global Pediatric Health and Equity: Solutions Exist. International Journal of Environmental Research and Public Health, 15(1), 16.
Prospero, J. M., Ginoux, P., Torres, O., Nicholson, S. E., & Gill, T. E. (2002). Environmental characterization of global sources of atmospheric soil dust identified with the Nimbus 7 Total Ozone Mapping Spectrometer (TOMS) absorbing aerosol product. Reviews of Geophysics, 40(1), 2-1-2–31.
Querol, X., Tobías, A., Pérez, N., Karanasiou, A., Amato, F., Stafoggia, M., Pérez García-Pando, C., Ginoux, P., Forastiere, F., Gumy, S., Mudu, P., & Alastuey, A. (2019). Monitoring the impact of desert dust outbreaks for air quality for health studies. In Environment International, 130.
Rajabi, M., & Souri, B. (2014). Evaluation of heavy metals among dustfall particles of Sanandaj, Khorramabad and Andimeshk cities in western Iran 2012-2013. Iranian Journal of Health & Environment, 8(1), 11-21.
Rezazadeh, M., Irannejad, P., & Shao, Y. (2013). Climatology of the Middle East dust events. Aeolian Research, 10, 103–109.
Saeifar, M. H., & Alijani, B. (2019). Detection of Dust Storm Origins in the Middle East by Remotely Sensed Data. Journal of the Indian Society of Remote Sensing, 47(11), 1883–1893.
Satheesh, S. K., Deepshikha, S., & Srinivasan, J. (2006). Impact of dust aerosols on Earth-atmosphere clear-sky albedo and its short wave radiative forcing over African and Arabian regions. International Journal of Remote Sensing, 27(8), 1691–1706.
Tabatabaei, T., Karbassi, A.R., Moatar, F., Monavari, S.M. (2015). Geospatial patterns and background levels of heavy metal in deposited particulate matter in Bushehr, Iran. Arabian Journal of Geosciences 8, 2081-2093.
Thakur, M., Deb, M. K., Imai, S., Suzuki, Y., Ueki, K., and Hasegawa, A. (2004). Load of heavy metals in the airborne dust particulates of an urban city of central India. Environmental Monitoring and Assessment, 95(1-3), 257-268.
Tong, D. Q., Gill, T. E., Sprigg, W. A., Van Pelt, R. S., Baklanov, A. A., & Barker, B. M. (2023). Health and safety effects of airborne soil dust in the Americas and beyond. Reviews of Geophysics, 61, e2021RG000763.
Turekian, K. K., & Wedepohl, K. H. (1961). Distribution of the elements in some major units of the earth's crust. Geological Society of America Bulletin, 72(2), 175–192.

Wagner, S. (2009). Soil (chrono-) sequences on marine terraces pedogenesis in two coastal areas of Basilicata and Agrigent, southern Italy [dissertation]. Council of Natural Sciences Faculty, University of Hohenheim, Stuttgart, Germany.

Wang, X. M., Huang, N., Dong, Z. D., & Zhang C. X. (2010). Mineral and trace element analysis in dustfall collected in Hexi corridor and its significance as an indicator of environmental changes. Environmental Earth Sciences, 60(1), 1–10.

Wei, B. G., & Yang, L. S. (2009). A review of heavy metal contaminations in urban soils, urban road dusts and agricultural soils from China. Microchemical Journal, 94(2), 99–107.

Xi, X., & Sokolik, I. N. (2012). Impact of asian dust aerosol and surface albedo on photosynthetically active radiation and surface radiative balance in dryland ecosystems. Advances in Meteorology.

Xia, W., Wang, Y., Chen, S., Huang, J., Wang, B., Zhang, G. J., Zhang, Y., Liu, X., Ma, J., Gong, P., Jiang, Y., Wu, M., Xue, J., Wei, L., & Zhang, T. (2022). Double Trouble of Air Pollution by Anthropogenic Dust. Environmental Science & Technology, 56(2), 761-769.

Xuana, J., Sokolikb, I. N., Haoc, J., Guoc, F., Maoc, H., & Yang, G. (2004). Identification and characterization of sources of atmospheric mineral dust in East Asia. Atmospheric Environment, 38(36), 6239-6252.

Zamanian, K., Pustovoytov, K., & Kuzyakov, Y. (2016). Pedogenic carbonates: Forms and formation processes. In Earth-Science Reviews, 157.

Zarasvandi, A. L. (2013). Geochemical composition and source of dust storms particles in Khuzestan Province using REE geochemistry: Concerning on geo-environmental parameter. Proceedings of Conference of Dust Haze, Monitoring, Effects and Solutions; Tehran, Iran. (in Persian)

Zarasvandi, A., Rezaei, M., Raith, J. G., Asadi, S., & Lentz, D. (2019). Hydrothermal fluid evolution in collisional Miocene porphyry copper deposits in Iran: Insights into factors controlling metal fertility. Ore Geology Reviews, 105, 183-200

Zhang, Z., Weichenthal, S., Kwong, J. C., Burnett, R. T., Hatzopoulou, M., Jerrett, M., Donkelaar, A. van, Bai, L., Martin, R. V., Copes, R., Lu, H., Lakey, P., Shiraiwa, M., & Chen, H. (2021). Long-term exposure to iron and copper in fine particulate air pollution and their combined impact on reactive oxygen species concentration in lung fluid: a population-based cohort study of cardiovascular disease incidence and mortality in Toronto, Canada. International Journal of Epidemiology, 50(2).